

## Long-Term Simulation of Cross Shore Sediment Transport of Submerged Mudbank Induced by Tidal Current: A Parametric Study

<sup>1</sup>M.F. Ahmad, <sup>2</sup>M. Mamat, <sup>2</sup>S. Rizki, <sup>2</sup>I. Mohd, <sup>1</sup>K.B. Samo, <sup>1</sup>A.M. Muzathik

<sup>1</sup>Department of Maritime Technology, Faculty of Education Maritime and Science Marine,  
University Malaysia Terengganu, 21030 Kuala Terengganu, Malaysia

<sup>2</sup>Department of Mathematics, Faculty of Science and Technology,  
University Malaysia Terengganu, 21030, Kuala Terengganu, Malaysia

**Abstract:** A parametric study of cross-shore sediment transport of submerged mudbank was conducted. The hydrodynamic force governed solely by tidal currents and purely mud sediment were considered in this study. One dimensional numerical analysis comprises of shallow water model, suspended transport model and bed material conservation model was developed to investigate the morphological behaviour of idealised submerged mudbank under such hydrodynamic and sediment conditions. A series of tests were carried out for some benchmark problems such as wave propagation and hump morphodynamics to validate the accuracy of the numerical scheme used. The system of hydrodynamic equations was solved using the finite volume numerical scheme associated with approximate Roe's Riemann solver, a data reconstruction and slope limiter. It was found that the predicted morphological behaviours of the submerged mudbank under the cross-shore tidal current for a five year period behave similar trends for the specified cases where height of hump profiles are reduced at the top and increased at both sides. The decreasing or increasing of bed profile depends on hydrodynamic factor such as erosion rate and settling velocity.

**Key words:** Sediment transport • Shallow water equations • Morphodynamic • Approximate Roe's Riemann solver

### INTRODUCTION

An engineering appraisal is required for many engineering works within coastal, estuarine or inland water such as dredging to sustain accessibility of navigation channel. The determination of the behaviour of sediment and prediction of sediment movement due to hydrodynamic forces are very important. Long-shore and cross-shore sediment transport due to currents and waves are responsible for many coastal engineering problems. Despite the extensive research over the past decades the process of the movement of this particular sediment and associated beach changes over the long term is still poorly understood. Sediment transport at a point in the near-shore zone is a vector with both long-shore and cross-shore components. For a number of coastal engineering scenarios of considerable interest, the transport is usually dominated by either the long-shore or cross-shore component and this, in part, has led to a

history of separate investigation efforts for each of these two components. The subject of total long-shore sediment transport has been studied for approximately five decade assuming cross-shore sediment transport is relatively small [1].

The role of cross-shore tidal currents or tidal waves is important to determine the morphological changes of the bed. The systematic study of the morphology of sandy bed is enormous but much less so for pure muddy bed. A number of systematic studies have been conducted to determine which forms of external forces are responsible for developing and maintaining the observed equilibrium morphologies for muddy bed [2-4]. Recently, INTRMUD (Inter-tidal mud) project on inter-tidal mudflat funded by the European Commission has been carried out with the aim to clarify the properties of the sediment, understand the mechanisms by which it is transported and clarify how the flat morphology varies with factors such as the tidal regime and the sediment properties and

supply. The aim of this study is to investigate the morphodynamics behaviour of hump sediment beds over an extended period of time. To achieve this aim, the specific objectives are as follow: (1) To develop a numerical scheme to study the long term behaviour of sediment humps consisting of mud; and (2) To analyze the morphological behaviour of the humps under tidal currents and sediment properties.

**Methodology:** The implementation of numerical scheme was applied to the shallow water model, sediment transport model and bed level evolution model. The shallow water model was balanced prior the numerical method and then the Godunov approach associated with approximate Roe's scheme solver, a balance technique a data reconstruction and slope limiter were used. To verify the numerical scheme for hydrodynamic the standard tidal wave propagation problem was compared. Besides that for morphodynamics verification, the shallow water model was decoupled with bed evolution model and tested by using the same approach. Later the idealised situation of humps beds comprises of mud was adopted to investigate their long term morphological behaviours. In this case, the suspended sediment transport model was coupled shallow water model whereas bed evolution was solved separately. A forward-difference scheme was used to solve bed level model to obtain the bed changes. A parameterization study was conducted to gain insight in the physical process of the flow and sediment transport.

**Set-up of Process-based Models:** A set-up of the process-based models developed in this work. The process-based models which are based on the hydrodynamic model, the sediment transport model and bed evolution model together with simplifications and assumptions are discussed.

**Hydrodynamic Model:** Cross-shore tidal current was considered as the main driving force for sediment transport. The assumption implies the model is only applicable to areas which are protected from big waves by either man-made structures or natural obstructions. In the conservation of momentum equation (2), a bottom stress model was included to represent the frictional effect of the bed on the flow. Other effects such as Coriolis, turbulent stresses, wind stress, atmospheric pressure at the water surface were ignored.

Under above assumptions, the mass and momentum conservation equations can be written as:

$$\frac{\partial h}{\partial t} + \frac{\partial(hu)}{\partial x} = 0. \quad (1)$$

$$\frac{\partial(hu)}{\partial t} + \frac{\partial\left(hu^2 + g\frac{h^2}{2}\right)}{\partial x} + gh\frac{\partial z_b}{\partial x} = \frac{-\tau_{bx}}{\rho} \quad (2)$$

where  $x$  = spatial coordinate;  $h$  = water depth;  $t$  = times;  $u$  = depth average velocity;  $z_b$  = bed elevation;  $g$  = gravity acceleration;  $\rho$  = water density;

$$\tau_{bx} = C_d u^2 \quad (3)$$

**Suspended Sediment Transport Models:** One dimensional concentration sediment transport without the diffusion term was implemented in this study assuming that the diffusion process was less significant than the advection process. The concentrations of mud using the suspended sediment transport equations is shown as

$$\frac{\partial}{\partial t}(hc_m) + \frac{\partial}{\partial x}(U_x hc_m) = E_m - D_m \quad (4)$$

where  $h$  = total water depth; and  $U_x$  = depth average velocity in  $x$ -direction;  $c_m$  = mud concentrations;  $D_m$  = mud deposition,  $E_m$  = mud erosion rates;

$$D_m = w_m c_m \left[ 1 - \frac{\tau_b}{\tau_d} \right] \quad (5)$$

where  $w_s$  = settling velocity for sand;  $w_s$  = settling velocity for mud;

$$E_m = P_m M_m \left[ \frac{\tau_b}{\tau_{e,c}} - 1 \right] \quad (6)$$

where  $P_m$  = percentage of mud;  $M_m$  = erosion rate for mud;  $\tau_b$  = bed shear stress; and  $\tau_{e,c}$  = critical shear stress.

The mud content ( $P_m$ ) defined as the percentage of mud content in the bed sediments was included in the model. The mud content was assumed to be constant, thus at every time step, when process of erosion occurs, the same proportion of sand and mud will be eroded and entrained into the water column.

**Bed Level Model:** Since the seabed in this study was purely mud, therefore, the bed-load transport was ignored.

The bed level changes were modelled through the sediment budget equation which describes the evolution of the bed level as.

$$\frac{\partial z_b}{\partial T} = \frac{D - E}{1 - p} \quad (7)$$

where  $D$  = deposition fluxes,  $E$  = erosion fluxes;  $p$  = bed porosity and  $z_b$  = bed level.

In this work, equation (7) was applied in simulations of purely mudbank. Bed porosity was assumed to be constant with time and space and take a value of 0.4.

**Numerical Implementation - Godunov Approach of Finite Volume Method:** The application of Roe's Riemann solvers, data reconstruction and balancing of flux gradient and source terms are described.

**The Flux of Roe's Riemann Solver as Follows:**

$$F_{i+1/2} = \frac{F_L + F_R}{2} - \frac{1}{2} \sum_{p=1}^m \tilde{\lambda}^{(p)} \tilde{\alpha}^{(p)} \tilde{K}^{(p)} \quad (8)$$

were  $\tilde{\alpha}^{(p)}$  = wave strength;  $\tilde{\lambda}^{(p)}$  = eigenvalues;  $\tilde{K}^{(p)}$  = right eigenvectors.

A new value of the conserve variable can be determined with the equation.

$$U_i^{n+1} = U_i^n + \frac{\Delta t}{\Delta x} [F_{i-1/2} - F_{i+1/2}] \quad (9)$$

MUSCL can be obtained by reconstructing the data and nonlinear slope limiter version was used to prevent unphysical oscillations. This will render the scheme to total variation diminishing (TVD). Herein, the limiter was

implemented such that, for consecutive cells  $i-1$ ,  $i$ ,  $i+1$  on a locally uniform grid, the reconstructed Riemann states were given by Roger [5] as.

$$u_i^L = u_i(0) = u_i^n - \frac{1}{2} \Phi_i \Delta_{i-1/2}; \quad u_i^R = u_i(\Delta x) = u_i^n + \frac{1}{2} \Phi_i \Delta_{i-1/2} \quad (10)$$

The slope limiter  $\Phi$ , proposed by Hirsch [6] was used in the simulations. It is defined as.

$$\Phi(r) = \max[0, \min(\beta r, 1), \min(r, \beta)], \quad (11)$$

where the limiter parameter  $1 \leq \beta \leq 2$  and the gradient ratio is given by

$$r = \begin{cases} \frac{u_{i+1} - u_i}{u_i - u_{i-1}}, & u_i - u_{i-1} \neq 0, \\ 0, & u_i - u_{i-1} = 0 \end{cases} \quad (12)$$

The choice  $\beta 1.5$  was used in the slope limiter.

A numerical imbalance is created by the artificial splitting of physical term  $gh \frac{\partial \zeta}{\partial x}$  to gives the flux gradients and source terms [7] as

$$gh \frac{\partial \zeta}{\partial x} = \frac{\partial}{\partial x} \left( \frac{1}{2} gh^2 \right) + gh S_{ox} \quad (13)$$

(surface gradient term flux gradient term + source term),

where  $g$  = gravitational acceleration;  $h$  = total water depth;  $\zeta$  = water surface  $S_{ox}$  = bed slope in  $x$  - direction.

According to Roger *et al.* [7] the numerical difficulties arise with the splitting in the equation (13) if non-uniform bathymetries are accounted such as in the case of wave propagation in this study. To avoid this problem, a technique suggested by Roger *et al.*, [7] was used.

Therefore the modified equations in vector form are written as:

$$\frac{\partial}{\partial t} \begin{bmatrix} \zeta \\ uh \\ hc_m \end{bmatrix} + \frac{\partial}{\partial x} \left[ u2h + \frac{1}{2} \frac{uh}{huc_m} (\zeta^2 + 2\zeta h_s) \right] = \begin{bmatrix} - \left( gh \frac{\partial z_b}{\partial x} - g h_s^0 \frac{\partial z_{b,s}}{\partial x} \right) \\ - C_d u^2 \end{bmatrix} \quad (14)$$

where subscript  $m$  as mud.

**Eigenstructure in Terms of Conserved Variables:** The Jacobian matrix (A), eigenvalues and eigenvectors are:

$$A = \begin{bmatrix} 0 & 1 & 0 \\ a_2 - \tilde{u} & 2\tilde{u} & 0 \\ -\tilde{u}c & c & \tilde{u} \end{bmatrix}, \lambda_1 = \tilde{u} - a, \lambda_2 = u, \lambda_3 = \tilde{u} + a \quad (15)$$

The wave strength of  $\tilde{a}_1, \tilde{a}_2$  and  $\tilde{a}_3$  are given as

$$\tilde{a}_1 = \frac{\Delta u_1(\tilde{u} + a) - \Delta u_2}{2a}, \tilde{a}_2 = \Delta u_3 - c\Delta u_1, \tilde{a}_3 = \frac{\Delta u_1(\tilde{u} - a) - \Delta u_2}{2a} \quad (16)$$

where

$$\begin{aligned} \Delta u_1 &\equiv \zeta_R - \zeta_L \\ \Delta u_2 &\equiv u_R h_R - u_L h_L \text{ or } q_R - q_L \\ \Delta u_3 &\equiv u_R c_R - h_L c_L \end{aligned} \quad (17)$$

**Discretization for source term (S')**: The source terms were evaluated in a pointwise manner and difference scheme was used to discretize the spatial gradients of bed elevation at node  $i$ .

$$S' = \left[ - \left( gh \frac{\partial z_b}{\partial x} - g h_s \frac{\partial z_{b,s}}{\partial x} \right) - C_d u^2 \right] = \left[ - \frac{1}{\Delta x} (g)(z(i) \left( \frac{b(i+1) - b(i-1)}{2} \right) - C_d |u_i| u_i) \right] \quad (18)$$

**Discretization for Bed Evolution Model:** The bed level model from equation (7) was applied to determine bed level changes and an explicitly different scheme was used to discretize this equation. It is given as

$$z_b^{n+1} = z_b^n - \frac{1}{1-p} \Delta t (D - E)_i^n \quad (19)$$

## RESULTS AND DISCUSSION

In order to verify the numerical scheme, tidal wave propagation with underneath of uneven bottom [8] and 1-D channel problems [9] were selected.

**Numerical Results:** In tidal wave propagation problem, Figure 1.0 and Figure 2.0 illustrate the results of and velocity ( $u$ ) and surface elevation ( $h$ ) after  $t=10800$ s using finite volume numerical scheme respectively. The information of surface elevation (Figure 1.0) and velocity

(Figure 2.0) are correct as expected at time 10800s. No waves propagate after the distance of 216000 m. It seems that by using the method of data reconstruction with slope limiter and balance the equation prior the uses of numerical scheme work very well with Roe approximation Riemann solver.

In 1-D channel problem, a small hump on the bottom bed is interacting slowly with the water flow where  $A = 0.001$  and  $Q_c = 10$ . Figure 3.0 illustrates the results obtained using the numerical scheme and approximate solution at  $t = 238079$  seconds. To ensure the scheme is stable,  $\Delta t = 0.1$  seconds and  $\Delta x = 2.5$  were chosen. As shown in the Figure 7, the maximum different between numerical scheme and approximate solution [9] is  $7.7 \times 10^{-4}$  for the bed bathymetry. From this result, it seems that the numerical scheme and the balancing of the flux gradient and source term technique prior numerical scheme can be used for investigation the behaviour mudbank.

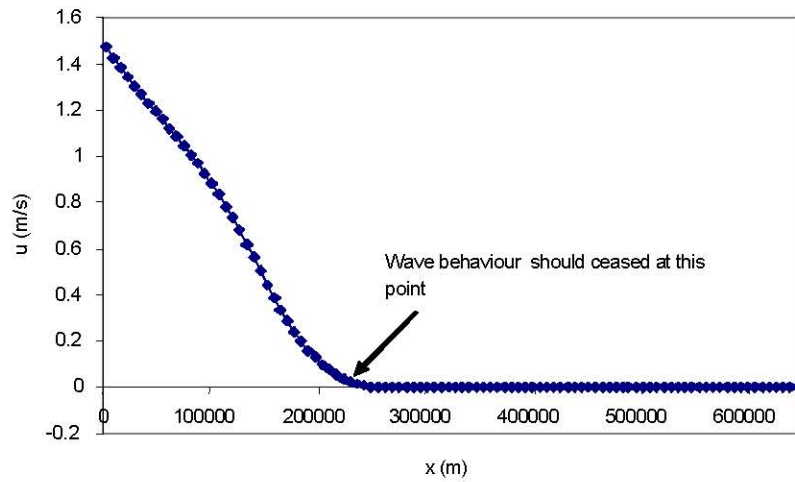


Fig. 1.0: Velocity at  $t = 10800$ s

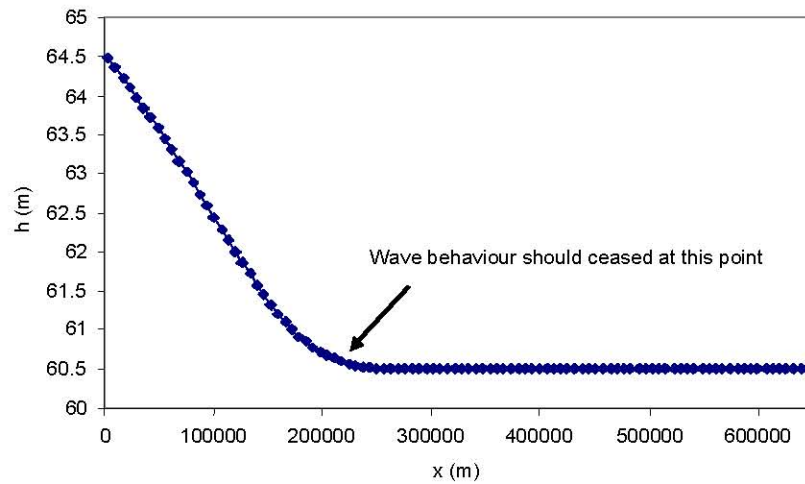


Fig. 2.0: Water level at  $t = 10800$ s

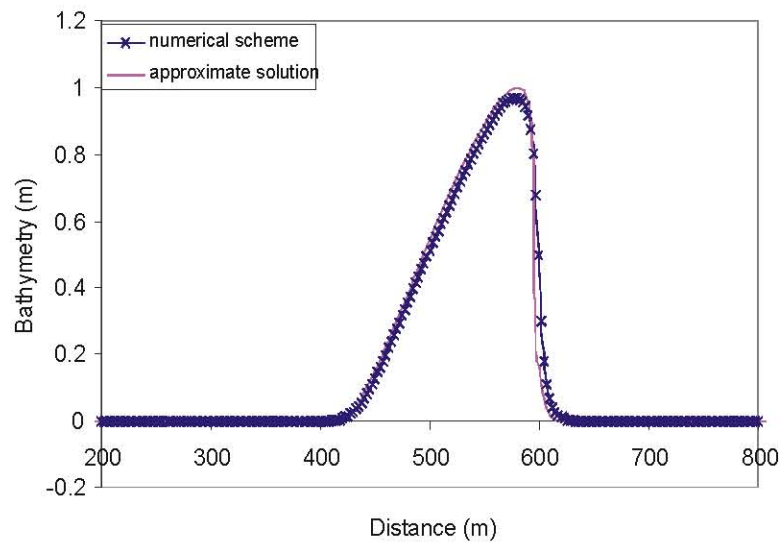


Fig. 3.0: Comparison of the numerical scheme and approximate solution with  $A = 0.001$  and  $Q_c = 10$  at  $t = 238079$ s.

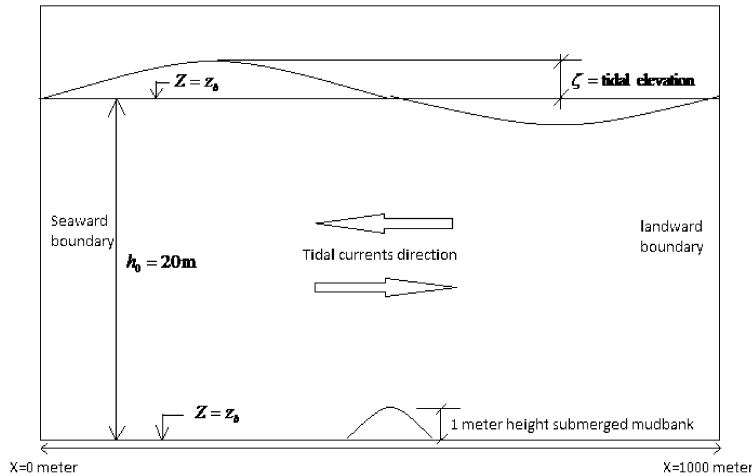


Fig. 4.0: Model set-up of mud bank

### Parametric Study -Purely Mudbank Cases

**Model Set-up:** An idealised situation where only one single hump so called submerged mudbank on the seabed was chosen as a study case for investigating the behaviour of the sediment transport. In this work, the submerged mudbank consisting of single fraction of purely mud was considered. The case was selected due to existence of the particular condition commonly found along the coast of North Africa where the sediment covered almost by mud.

**Geometry:** A physical domain was simplified to represent the idealised situation as shown in Figure 4.0. The domain has a length of 10000 meter which seaward end located at point  $x = 0$  meter and the landward end located at point  $x = L$  meter. The consolidated sediment bed profile is flat with a half sinusoidal shape in the middle of the domain represent as hump. The hump with 1.0 m in height is submerged in the water of 20 m in height ( $h_0$ ). The bottom bed ( $z = b_0$ ) is erodible and consists of pure mud sediments.

**Boundary Conditions:** The tidal was induced at  $x = 0$  meter by computing the variation of water level according to the equation (21). It seems that water motion is generated by external tidal motion at the seaside.

$$\zeta(t) = \zeta_0 \cos(\omega t) \quad (21)$$

where  $\zeta$  = water level;  $\zeta_0$  = tidal amplitude;  $\omega$  = tidal frequency =  $\frac{2\pi}{T}$  where  $T$  = Time (taken as 12 hours).

In this study the behaviour of the sediment transport was focused without considering the influence of concentration at the sea boundary. However, the concentration will occur when the process of erosion takes place on the bottom bed due to the excess bed shear stress relative to critical bed shear stress.

**Physical Parameters:** The settings for the physical parameters depend on case to be studied. Here, the bed was cohesive sand and mud mixture. The parameters are tabulated according to the cases as shown in the following sections. The parameters for sand and mud such as the critical deposition  $\tau_d$  and the settling velocity  $w_s$  were set as constant within a realistic range. A quadratic drag law was used to express the bottom friction with coefficient  $C_d$  being taken as constant.

**Numerical Parameters:** The horizontal grid size  $\Delta x$  was taken 200 meter and time step  $\Delta t$  for the water motion, suspended sediment transport and morphology was taken 12 seconds. The time step in bed level computation was multiplied by  $N$  where  $N$  was the morphological factor and was taken to be 60. This morphological factor implies that for a simulation of 12 tidal cycles, it actually represents the morphological change over one year [10].

**Case 1:** The settings for the physical parameters are tabulated in Table 1.0. It should be noted that the erosion rates were set with different values for each test. The tests investigated the sensitivity of the model behaviour due to the erosion rate. The critical shear stresses for erosion ( $\tau_{c,e}$ ), the critical shear stress for deposition ( $\tau_{c,d}$ ),

Table 1.0: Parameters settings for pure mud (Case1)

	Parameter				
Drag coefficient, $C_d$ (dimensionless)	0.002	0.002	0.002	0.002	0.002
Constant rate erosion, $M_e$ (kg/m <sup>2</sup> /s)	$2e^{-7}$	$4e^{-7}$	$6e^{-7}$	$8e^{-7}$	$1e^{-6}$
Critical erosion mud, $\tau_{c,e}$ (N/m <sup>2</sup> )	0.2	0.2	0.2	0.2	0.2
Critical deposition mud, $\tau_{c,d}$ (N/m <sup>2</sup> )	0.2	0.2	0.2	0.2	0.2
Settling velocity of mud, $w_s$ (m/s)	0.005	0.005	0.005	0.005	0.005
Percentage of mud, $P_m$ (%)	100	100	100	100	100
Tidal height (m)	1.1	1.1	1.1	1.1	1.1

the settling velocity ( $w_s$ ) and tidal height ( $\zeta_0$ ) were taken similar for all tests. The simulations were taken for five years to determine the morphology behaviour of the purely mud bed.

The observed morphological behaviour as shown in Figure 5.0 indicates that the erosion rate plays a significant role in determining the morphological behaviour for a pure mud bed. With the same parameters settings throughout the tests, erosion rate of  $1.0e^{-6}$  kg/m<sup>2</sup>/s contributes more erosion relative to other erosion rates. Smallest quantity of eroded sediment corresponds to the erosion rate of  $2e^{-7}$  kg/m<sup>2</sup>/s. The eroded sediment is brought into suspension by the horizontal velocity (tidal current) and deposit at both sides of the hump where the bed shear stress for deposition is lesser than critical deposition rate. The quantity of sediment lost at the top of hump is balanced by the quantity of sediment deposits at  $\pm 5$  percent compared to the initial bed profile. The models are sensitive to the erosion rate and produce the difference of predicted profiles on each test but the

Table 2.0: Parameters settings for pure mud (Case 2)

	Parameter		
Drag coefficient, $C_d$ (dimensionless)	0.002	0.002	0.002
Constant rate erosion, $M_e$ (kg/m <sup>2</sup> /s)	$1e^{-6}$	$1e^{-6}$	$1e^{-6}$
Critical erosion mud, $\tau_{c,e}$ (N/m <sup>2</sup> )	0.2	0.2	0.2
Critical deposition mud, $\tau_{c,d}$ (N/m <sup>2</sup> )	0.2	0.2	0.2
Settling velocity of mud, $w_s$ (m/s)	0.001	0.01	0.1
Percentage of mud, $P_m$ (%)	100	100	100
Tidal height, $\zeta$ (m)	1.1	1.1	1.1

profile shapes remain the same. From Figure 10.0, it seems the models behave as expected with the constant erosion rate of the beds.

**Case 2:** The settings for the physical parameters are tabulated in Table 2.0. It should be noted that the settling velocities,  $w_s$  were set as different value for each test. The aim was to investigate the sensitivity of the model behaviour due to the settling velocity. The critical shear stresses for erosion  $\tau_{c,e}$ , the critical shear stress for deposition  $\tau_{c,d}$ , the erosion rate  $M_e$  and tidal height  $\zeta_0$  were taken similar for all tests.

Figure 6.0 shows the results of predicted mud bed profiles to investigate the effect of the settling velocity on the shape of the hump. The settling velocity values were varied between 0.001 to 0.1 m/s. It can be seen that the calculated mud bed profiles are different at both sides of the hump with the different of settling velocities. However, at the top of the hump the difference of the profiles are not significant. On the right hump, the settling velocity 0.1 m/s gives an offset of the shape of the hump relatives to the initial profile and high bed profile from

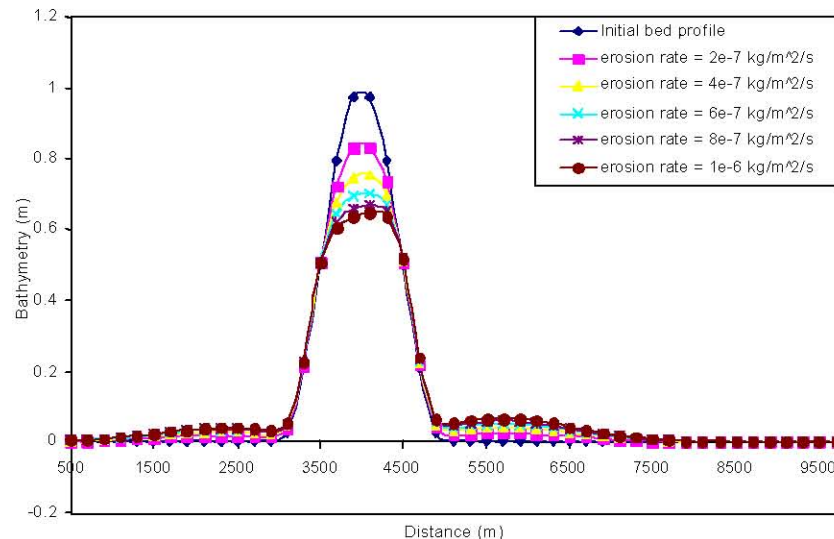


Fig. 5.0: Mud bed profile after 5 years simulations with different erosion rates (Case 1)



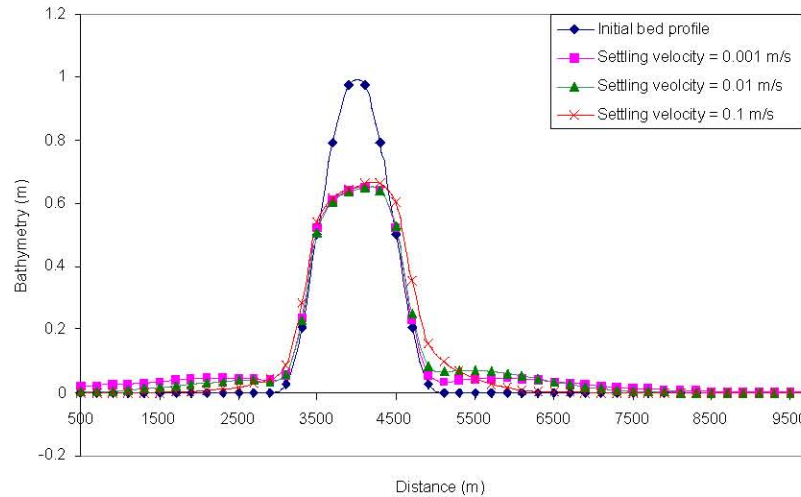


Fig. 6.0: Mud bed profiles after 5 years with different settling velocity (Case 2)

5000 m to 5500 m. After the distance of 5500 m, this settling velocity produces the lowest bed profile. These calculated bed profiles are consistent with the formation of biggest floc occurring and leading to a fastest deposition. The deposition process of sediment is concentrated very much within that particular distance and balance of sediment in term of quantity leaves little to deposit after 5500 m. The sediment deposits on left side of the hump are due to the reverse flows (ebbs). At this side the predicted bed profiles show decreasing in profiles as the velocity increases. This could be explained that the tidal currents transport less quantity of sediment to the left side after heavy deposition process happened on the right side of the hump. Therefore, a high value of settling velocity does not necessarily give a strong deposition process and it will also depend on the shape of bottom profile.

### CONCLUSION

For investigation of the morphological behaviour of hump bed under the cross-shore tidal current, a one dimensional numerical model based on the shallow water equations, suspended sediment transport formulae and bed material conservation equation were developed. The standard benchmark test problem of tidal wave propagation was used to test the schemes. The scheme that is found to be accurate based on the finite volume approach associated with approximate Roe's Riemann solver. A balance technique is applied to modify the original shallow water equations combined with a data reconstruction and slope limiter also increases the accuracy of the results. The hydrodynamic model was

coupled with the sediment transport and applied bed level model to produce the morphodynamic model. The accuracy of the morphodynamic model has been confirmed through the study of morphological changes for idealised situations in Hudson and Sweby [9]. In this the morphological behaviours of the hump mudbank showed that the height of hump profiles are reduced at the top and increased at the both sides under the tidal current in the period of five year. The amount of decreasing and increasing of bed profiles depend on sediment parameters such as erosion rate and settling velocity.

### REFERENCES

1. Dean, R.G., 1995. *Advances in coastal and ocean engineering*. World Scientific.
2. Dyer, K.R., 1998. The typology of intertidal mudflats', in K. Black et al., (eds.), *Sediment Processes in the Intertidal Zone*. London: Geo. Soc.
3. Kirby, R., 2000. Practical implications of tidal flat shape', *J. Continental Shelf Res.*, 20: 1061-1077.
4. Pritchard, D. and A.J. Hogg, 2003. Cross-shore sediment transport and the equilibrium morphology of mudflats under tidal currents, *J. Geophysical Res.*, 108(C10): 11(1-15).
5. Roger, B.D., M. Fujihara and A.G.L. Borthwick, 2001. 'Adaptive Q-tree Godunov-type scheme for shallow water equations', *International J. for Numerical Methods in Fluids*, 35: 247-280.
6. Hirsch, H., 1990. *Numerical computation of internal and external flows*, Vol. 2. *Computational Methods for Inviscid and Viscous Flows*. New York.



7. Roger, B.D., A.G.L. Borthwick and P.H. Taylor, 2003. Mathematical balancing of flux gradient and source terms prior to using Roe's approximate Riemann solver, *J. Computational Physics*, 192: 422-451.
8. Bermudez, A. and M.E. Vazquez, 1994. Upwind methods for hyperbolic conservation laws with source terms, *J. Computers Fluids*, 23(8): 1049-1071.
9. Hudson, J. and P.K. Sweby, 2003. Formulations for numerically approximating hyperbolic systems governing sediment transport, *J. Sci. Computing*, 19: 225-252.
10. Ahmad, M.F., 2008. Tidally induced cross shore sand mud transport and long term bed profile evolution. Thesis of PhD, Division of Civil Engineering, School of Engineering, Physics and Mathematics, Dundee University.